

# Combined -Pirani/bending membrane- pressure sensor

Category: Sensors

J.J. van Baar, R.J. Wiegerink, T.S.J. Lammerink, E. Berenschot, G.J.M. Krijnen  
and M. Elwenspoek

MESA Research Institute, University of Twente  
P.O. Box 217, 7500 AE Enschede, The Netherlands  
e-mail: J.vanBaar@el.utwente.nl fax: +31-53-489 3343

## Abstract

A differential pressure sensor has been realized with thermal readout. The thermal readout allows simultaneous measurement of the membrane deflection due to a pressure difference and measurement of the absolute pressure by operating the structure as a Pirani pressure sensor.

## Introduction

Two distinct classes of pressure sensors are formed on one hand by bending membrane pressure sensors, where a pressure difference results in a membrane deflection, and on the other hand by thermal pressure sensors, where the thermal conductivity of a gas is used as a measure for the absolute pressure [1]. In this paper a sensor is presented, which combines these two measurement principles. As a result, the sensor can be used for simultaneous measurement of the pressure difference and the absolute pressure.

In the case of bending membrane pressure sensors, the membrane deflection is usually measured using a change in electrical capacitance or by integrating strain gauges in the membrane. An alternative is to measure the thermal conductance between the membrane and a heat sink, the silicon substrate, placed at a close distance. This was demonstrated in [2], where a heater was integrated on the membrane and the membrane temperature was measured using thermo-piles. The heat sink was realized by bonding a second wafer on top of the wafer containing the membrane. The distance between the heated membrane and heat sink was in the order of 10  $\mu\text{m}$ .

The sensor presented in this paper has a much smaller distance between membrane and heat sink, which is essential for using the structure to measure absolute pressure levels around atmospheric pressure. Furthermore, the sensor can be realized in a simple and reliable fab-

rication process based on etching of a sacrificial poly-Si layer between two silicon nitride layers [5].

## Operation principle

Figure 1 shows the basic structure of the sensor. It consists of a circular silicon nitride membrane positioned 1  $\mu\text{m}$  above the silicon substrate. A channel connects the cavity below the membrane with a hole at the backside of the wafer. Thus, a pressure difference between the front and backside of the wafer causes the membrane to bend. A platinum resistor is integrated on top of the membrane and acts both as heater and as temperature sensor. An identical platinum resistor on the substrate is used as a reference sensor. When the membrane is heated by a constant current through the electrical resistor the resulting membrane temperature, with respect to the substrate, is dependent on both the distance from the substrate, i.e. the membrane deflection, and the pressure dependent thermal conductivity of the medium between the membrane and substrate. In principle the thermal readout is suitable for operation at high temperatures, because the temperature difference between the membrane and the substrate is measured, which is in first order approximation independent of the absolute temperature [3]. The deflection of the membrane and the dependency of the thermal conductivity on pressure are depicted in figures 2 and 3.

The thermal resistance between the heated membrane and the substrate can be expressed by:

$$\frac{\Delta T}{Q} = R_{therm} = \frac{l}{\kappa A} \quad (1)$$

with  $\kappa_f$  [ $\text{W}/(\text{Km})$ ] the thermal conductivity of the medium,  $l$  [ $\text{m}$ ] the gap distance and  $A$  [ $\text{m}^2$ ] the area of the membrane. A heating power  $Q$  [ $\text{W}$ ] can be applied, which results in a temperature difference  $\Delta T$  [ $\text{K}$ ] and gives the thermal resistance  $R_{therm}$  [ $\text{K}/\text{W}$ ].

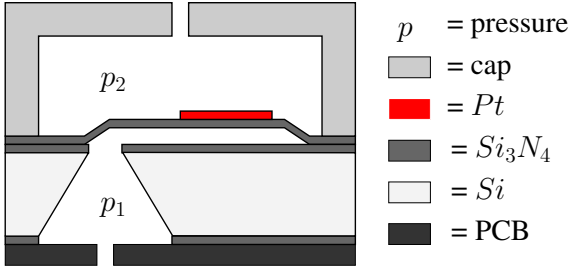


Figure 1: Schematic drawing of the structure

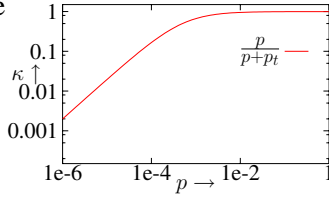


Figure 2: Normalized thermal conductivity versus normalized pressure

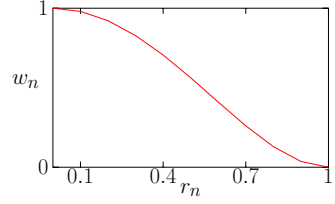


Figure 3: Normalized deflection versus normalized radius

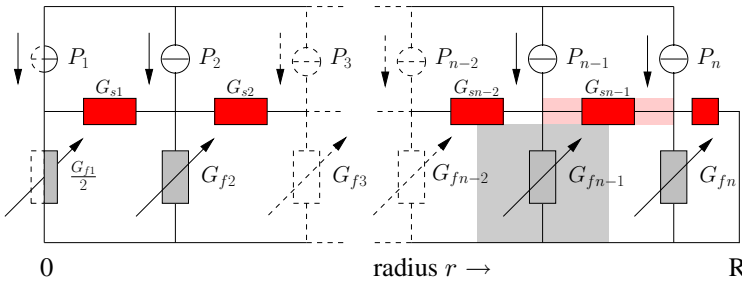


Figure 4: Lumped element model used for calculating the temperature distribution of a deflected membrane.

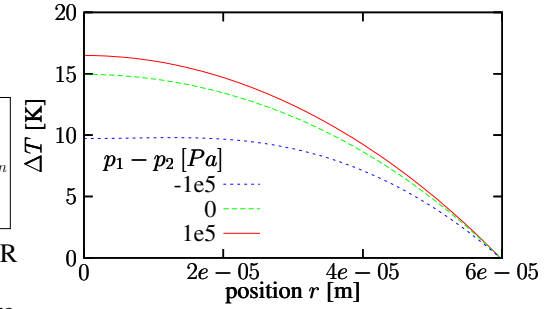


Figure 5: Calculated temperature distribution

The temperature distribution over the membrane is defined by the ratio between the heat transport through the medium and the heat transport through the membrane to the edge of the membrane. The temperature distribution can be obtained by solving the following one dimensional differential equation:

$$-h\kappa_s \left( \frac{d^2 T}{dr^2} + \frac{1}{r} \frac{dT}{dr} \right) + \frac{\kappa_f}{l} T = Q'' \quad (2)$$

with  $\kappa_s$  and  $\kappa_f$  the thermal conductivity of the solid membrane and fluid, respectively, and  $Q'' [W/m^2]$  the applied heating power per area.

Using the boundary conditions  $T(R) = 0$  and  $\frac{T(0)}{dr} = 0$  and taking for the thermal square conductance  $G_f'' = \frac{\kappa_f}{l} [W/(Km^2)]$  and the thermal square resistance of the membrane  $R_s'' = \frac{1}{\kappa_s h} [K/W]$  the solution becomes:

$$T(r) = \frac{Q''}{G_f''} \left( 1 - \frac{BesselJ_0 \left( r \sqrt{-G_f'' R_s''} \right)}{BesselJ_0 \left( R \sqrt{-G_f'' R_s''} \right)} \right) \quad (3)$$

This solution is plotted in figure 5 as the center curve with  $p = 0 [Pa]$ . When a pressure difference  $p_1 - p_2 [Pa]$  is applied over the membrane it will bend and the gap distance  $l$  changes. For a circular membrane with radius  $R [m]$  the deflection  $w [m]$  is given by [4]:

$$w(r) = \frac{3}{16} \frac{1 - \nu^2}{E h^3} (R^2 - r^2)^2 \cdot p \quad (4)$$

with  $\nu$  the Poisson ratio,  $E [Pa]$  the Young's modulus,  $h [m]$  the thickness,  $p [Pa]$  the pressure drop and  $r [m]$  the radius from the center of the membrane.

For a deflected membrane the differential equation 2 becomes nonlinear and is difficult to solve. Instead, the lumped element model, indicated in figure 4, was used to calculate the temperature distribution. In this model, the heat conductance through the membrane is represented by the conductances  $G_s [W/(Km)]$ . The heat conductance through the fluid to the substrate is modeled by the conductances  $G_f [W/(Km)]$ , which are dependent on the membrane deflection. The results are also shown in figure 5.

Due to the Pirani effect the thermal conductance of the fluid  $G_f$  becomes dependent on the pressure, when the distance between the heated membrane and the substrate is smaller than the mean free path of the gas molecules. Around atmospheric pressure this effect becomes noticeable when the distance is in the order of  $1 \mu m$ . The Pirani effect can easily be included in the lumped model by making the conductances  $G_f$  dependent on both the membrane deflection and the absolute pressure beneath the membrane.

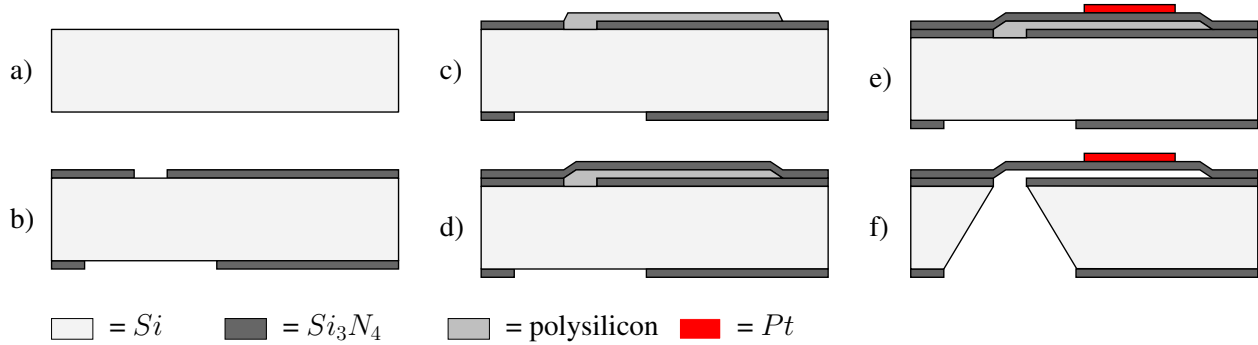


Figure 6: Process outline

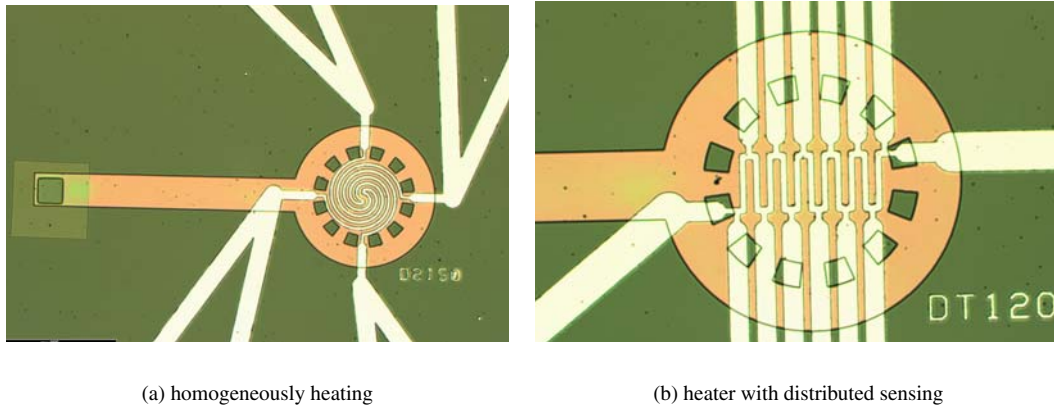


Figure 7: Photographs of two types of pressure sensors

## Fabrication process

In [5] a sacrificial poly-Si layer of about 1 mm long and 1  $\mu\text{m}$  high between two silicon nitride layers was etched open by KOH etching from the backside of the wafer. In this way we have realized silicon nitride membranes on the surface of the wafer with the cavity between it connected by a channel to the etch opening at the backside of the wafer. The hole on the backside can easily be closed or connected to a tube. An important advantage compared to other sacrificial layer processes is that it is not necessary to seal etching channels needed to have access to the sacrificial layer.

The diameter of the membrane is 120  $\mu\text{m}$  (largest type was 240  $\mu\text{m}$ ) and the thickness is 1  $\mu\text{m}$ . This is placed above a heat sink with a gap of 1  $\mu\text{m}$ . The metal heater/sensor on top of the membrane consists of a 10 nm Cr adhesion layer and a 200 nm Pt layer, with a width of 5  $\mu\text{m}$ , a curved length of 6 mm and a gap distance of

2.5  $\mu\text{m}$ . Note that the same fabrication process can be used to realize a strain gauge or capacitive readout simply by changing the platinum pattern. Different readout principles can even be combined on a single chip.

Figure 6 shows a summary of the fabrication process. On a bare silicon  $\langle 100 \rangle$  wafer (a) a 1  $\mu\text{m}$   $\text{Si}_3\text{N}_4$  layer has been deposited and patterned on both sides (b). A sacrificial 1  $\mu\text{m}$  polysilicon layer is used for defining the gap (c). On this an 1  $\mu\text{m}$   $\text{Si}_3\text{N}_4$  layer is deposited, which forms the membrane (d). The 10 nm Cr adhesion layer and the 200 nm Pt has been sputtered and lift-off has been used (e). The last step is the etching in KOH (f).

In figure 7 two types of pressure sensors are shown: one with homogeneous heating and the other with a meandering heater. The latter makes it possible to measure the temperature distribution. The measuring of the temperature distribution of a Pirani sensor and a flow sensor is presented in [6]. Only on the first type measurements have been carried out.

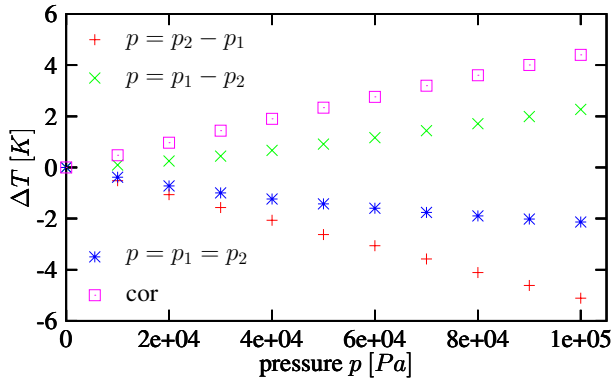


Figure 8: Measured temperature change as a function of the pressure drop applied over the membrane

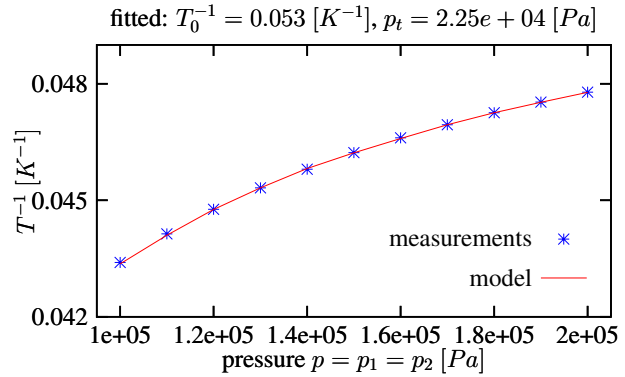


Figure 9: Thermal conductivity depending on the pressure, which applied on both sides of the membrane

## Measurements

The membrane was heated with a constant current of 4.5 mA and the resistance of the heater was approximately 600  $\Omega$ . The temperature was measured as a function of the pressure that was applied above  $p_2 - p_1$ , below  $p_1 - p_2$  or at both sides  $p = p_1 = p_2$  of the membrane. For curve  $p_2 - p_1$  we see that the temperature decreases almost linearly with increasing pressure. In this case the pressure between the membrane and substrate remains constant and the Pirani effect can be neglected. When the same pressure is applied on both sides of the membrane, curve  $p = p_1 = p_2$ , the membrane will not deflect. In this case we see that again the temperature decreases with increasing pressure, however the effect is nonlinear because for the gap distance of 1  $\mu\text{m}$  the Pirani effect decreases significantly around atmospheric pressure. A smaller gap distance will result in a much larger and more linear Pirani effect. When the pressure is applied below the membrane, curve  $p_1 - p_2$ , we have a combination of the Pirani effect, which causes a decrease of the temperature, and an upward deflection of the membrane, which causes an increase of the temperature due to the larger distance from the substrate. Correcting curve  $p_1 - p_2$  for the change in thermal conductivity  $p = p_1 = p_2$  gives curve *cor*. The latter is (apart from the sign) almost identical to  $p_2 - p_1$  showing that the membrane deflection is symmetrical.

For figure 9 the temperature difference of 23 K between the heater and sensor at atmospheric pressure has been taken and added to curve  $p = p_1 = p_2$  of figure 8. The reciprocal of this value has been taken, which is proportional to the thermal conductivity. A first order model has been fitted, which results in the transition pressure  $p_t$  [Pa] of about 0.2 bar.

## Conclusions

A combined Pirani/bending membrane pressure sensor has been realized. First measurement results show that the sensor is sensitive to both a pressure difference (causing a deflection of the membrane) and the absolute pressure between the membrane and the substrate.

## Acknowledgment

This research was funded by the Dutch Technology Foundation (STW).

## References

- [1] O. Paul. Vacuum gauging with complementary metal-oxide semiconductor microsensors. *J. Vac. Sci. Technol.*, A 13(3):503–508, 1995.
- [2] U.A. Dauerstadt, C.M.A. Ashruf, and P.J. French. A new high temperature pressure sensor based on a thermal read-out principle. *Transducers*, pages 525–530, 1999.
- [3] M. von Pirani. Selbstzeigendes vakuum-mesinstrument. *Verhandlungen der Deutschen Physikalischen Gesellschaft*, pages 686–694, 1906.
- [4] M. Elwenspoek and R.J. Wiegerink. *Mechanical microsensors*. Springer Verlag, 2000.
- [5] Xing Yang, Yu-Chong Tai, and Chih-Ming Ho. Micro bellows actuators. *Transducers*, pages 45–48, 1997.
- [6] J.J. van Baar, R.J. Wiegerink, T.S.J. Lammerink, G.J.M. Krijnen, and M. Elwenspoek. Micro-machined structures for thermal measurements of fluid and flow parameters. *JMM*, volume 11, issue 4 (July):311–318, 2001.